RESEARCH ARTICLE

Equal mixing time enables scale-down and optimization of a CHO cell culture process using a shaken microbioreactor system

Vincent Wiegmann[1] | Richard A. Gardner[2] | Daniel I. R. Spencer[2] | Frank Baganz[1]

[1] The Advanced Centre for Biochemical Engineering, Department of Biochemical Engineering, University College London, Gordon Street, London, WC1E 6BT, UK

[2] Ludger Ltd, Culham Science Centre, Abingdon, Oxfordshire, UK

Correspondence
Frank Baganz, The Advanced Centre for Biochemical Engineering, Department of Biochemical Engineering, University College London, Gordon Street, London, WC1E 6BT, UK.
Email: f.baganz@ucl.ac.uk

Abstract

The advancement of microbioreactor technology in recent years has transformed early- and mid-stage process development. The monitoring and control capabilities of microbioreactors not only promote the quick accumulation of process knowledge but has also led to an increased scalability when compared to traditionally used systems such as shake flasks and microtitre plates. This study seeks to establish a framework for the micro-Matrix microbioreactor (Applikon-Biotechnology BV) as process development tool. Using the Dual Indicator System for Mixing Time, the system was initially characterized for mixing properties at varying operating conditions, which was found to yield mixing times between 0.9 and 41.8 s. A matched mixing time was proposed as scale-down criterion for an IgG4 producing GS-CHO fed-batch process between a 5 L stirred tank reactor (STR) and the micro-Matrix microbioreactor. Growth trends, maximum viable cell concentrations, final titre, and glycoprofiles were nearly identical at both scales. The scale-down model was then employed to optimize a bolus feeding regime using response surface methodology, which led to a 25.4% increase of the space-time yield and a 25% increase of the final titre. The optimized feeding strategy was validated at the small-scale and successfully scaled up to the 5 L STR. This work for the first time provides a framework of how the micro-Matrix microbioreactor can be implemented in a bioprocess development workflow and demonstrates scalability of growth and production kinetics as well as IgG4 glycosylation between the micro-Matrix and a benchtop-scale STR system.

KEYWORDS
CHO cell culture, design of experiment, high throughput, microbioreactor, mixing time characterization, scale down

1 | INTRODUCTION

Process development within today's bioprocessing industry increasingly employs microbioreactor systems for screening and optimization.[1] The smaller footprint of such instruments allows for a high degree of parallelization and the small working volumes dramatically reduce the running costs compared to conventional benchtop bioreactors. Additionally, the application of disposables further increases throughput by eliminating time-consuming setup and cleaning steps.[2] As a result of this high throughput, large amounts of data can be generated quickly, which can then be used for the analysis with advanced statistical tools such as Design of Experiment (DoE) and multivariate data analysis (MVDA) to rapidly understand and optimize a cultivation process.[3,4]

To leverage the findings made in the high throughput systems, scalability to the larger scale is pivotal. An important step in that direction was brought about by the advancements in sensor technologies. Disposable, precalibrated dissolved oxygen (DO) and pH sensors are now regularly employed in microbioreactors to enable monitoring and control of these parameters at the millilitre scale.[5] In addition to the standard culture parameters, hydrodynamic and mass transfer conditions should be similar across scales to guarantee an analogous process performance. To do so, a scaling criterion is defined and set to remain constant between different cultivation systems.[6]

The choice of scaling criterion is primarily dependent on the cultivation system and cell type in use. Microbial growth is more likely to be limited by the transfer of oxygen into the growth medium, which renders the volumetric mass transfer coefficient ($k_L a$) a suitable scale criterion for microbial fermentation processes. As mammalian cells require considerably less oxygen, the $k_L a$ is often not the limiting factor [7] and an alternative scale criterion might be more suitable.

A matched power per unit volume (P/V) is widely used for the scale translation of microbial and mammalian processes [8–10] as the P/V combines mass transfer and hydrodynamic conditions.[11] However, to experimentally determine P/V in shaken systems is associated with considerable experimental effort. Although several studies have focused on the characterization of the power consumption in shake flasks and microtitre plates,[11–14] many of the more specific microtitre plate versions have not yet been considered in the literature.

Finally, a constant mixing time can be used as an engineering basis for the process translation between small-scale and benchtop-scale cell culture systems. This parameter describes the time it takes for a system to reach a state of specified homogeneity after a perturbation has been introduced. The advantage of this scaling criterion is that a measure of the mixing time can be established with relatively little experimental effort irrespective of the mode of agitation. A constant mixing time has been shown to result in comparable growth and production kinetics between the μ24 microbioreactor and shake flasks [15] as well as microtitre plates and stirred tank bioreactors.[16]

As indicated, the fundamental differences between shaken and stirred bioreactors complicate a scale translation between such systems. This study devises a scaling strategy based on a constant mixing time and demonstrates the validity of the scale-down model in a high-throughput optimization and subsequent scale up of the optimized process. To the knowledge of the authors, this contribution presents the first detailed description of the scale translation between a shaken microbioreactor and a benchtop-scale stirred tank reactor for cell culture processes.

2 | MATERIALS AND METHODS

2.1 | Cell culture

2.1.1 | Subculture

For all cell culture experiments, an IgG4-expressing GS-CHO-CY01 line (Lonza, UK) was used. Cells were thawed and transferred to 49 mL of CD-CHO (Life Technologies, UK) containing 25 μM methionine sulphoximine (MSX) in a vented 250 mL shake flask (Corning Life Sciences, USA). Cells were expanded on an orbital shaker with 25 mm throw (Sartorius, UK) at 160 rpm, 37°C, and 5% CO_2 and passaged every 3–4 days. The inoculum was prepared after 12–14 days of pre-expansion from cell populations in the exponential growth phase. The seeding density of all cultivations was 3×10^5 cells mL^{-1}.

2.1.2 | 24 Standard round well plate (24 SRW) cultivations

A Micro-Flask lid with regular gas permeability (CR1524, Applikon-Biotechnology BV, The Netherlands) was used to cover the 24 SRW. Prior to inoculation, the lid was autoclaved and left in the laminar flow cabinet to dry and cool down for at least 2 h. 0.8 mL of cell suspension was then transferred to each well of the 24 SRW. The lid was placed on top of the 24 SRW and a Micro-Flask cover clamp (Applikon-Biotechnology BV, The Netherlands) was used to fixate the assembled plate on an orbital shaker with 25 mm throw (Sartorius, UK). The fed-batch cultivation was performed at 220 rpm, 37°C, and 5% CO_2. Sampling was done sacrificially every 2–3 days. As a result of the irregular evaporation across microtitre plates,[17] corner wells were sampled first, then wells positioned on the side of the 24 SRW, and lastly wells with a central location on the plate. The manufacturer of the Micro-Flask lid states an average evaporation rate of 30 μL d^{-1} per well. This liquid loss was counteracted through daily bolus additions of 30 μL deionized (DI) water.

2.1.3 | Micro-Matrix cultivations

The micro-Matrix feeding module was autoclaved and then fitted with single-use filter bars (Applikon-Biotechnology BV, The Netherlands).

To correct the pH offset, each well of the micro-Matrix cassette was filled with 2 mL of Phosphate Buffered Saline (PBS, Life-Technologies, UK). The cassette was then covered with the feeding module and mounted onto the micro-Matrix system. Without gas supply or heating, the pH was recorded for a minimum of 2 h. The pH of the PBS was measured with an offline pH meter (Mettler Toledo, Switzerland) and used to recalibrate the sensors of the micro-Matrix cassette. The PBS inside the wells was then removed before each well was filled with 4 mL of medium containing the inoculum. The liquid addition bottle of the micro-Matrix was then filled with 200 mL of base and all liquid addition lines were primed. All cultivations were performed at 250 rpm, 0.4 vvm max. gas flow, pH 7.2, DO 30%, and 37°C. The pH was controlled via automated additions of 0.75 M NaOH using the feeding module and overlay with CO_2. The DO was controlled through overlay of N_2 and compressed air. Gas blends of 5% CO_2 balanced with either N_2 or air were used to increase the CO_2-fraction of the inflowing gas. Samples were taken immediately after feeding. The sample volume was equal to the feed volume, so that the working volume remained constant throughout the experiment. Previous experiments showed an average evaporation rate of 50 μL d^{-1} per well. This was counteracted through daily bolus additions of 50 μL DI water.

2.1.4 | 5 L Stirred tank bioreactor (STR) cultivations

A BIOSTAT B-DCU (B. Braun Biotech, Sartorius, Surrey, UK) with a nominal volume of 5 L was used for cultivations at the benchtop-scale. The vessel was equipped with a down pumping 45° pitched blade impeller that was set to a rotational speed of 260 rpm. The STR was aerated continuously at a flow rate of 0.07 vvm through a ring sparger. The cells were inoculated in an initial working volume of 2.75 L. Through feed additions, the working volume reached a final value of about 4.1 L. The temperature was controlled at 37°C and the pH was controlled at 7.2 using additions of either 1 M NaOH or sparged CO_2. The DO was maintained at 30% by sparging either N_2 or compressed air / O_2. To increase the CO_2-fraction of the inflowing gas, the same gas blends were used as described for the micro-Matrix. Bolus additions of 10 mL 1% Antifoam C Emulsion (Sigma-Aldrich, UK) were added on a daily basis to the culture.

2.1.5 | Fed-batch strategy

In all cultivation platforms, CD-CHO without MSX was used as basal medium. The ratio of sample volume to working volume was higher in the micro-Matrix compared to the 5 L STR and the 24 SRW. To prevent overfeeding in the micro-Matrix cultures, the feed volume was based on the current working volume rather than the initial working volume. Bolus feeding of Efficient Feed B (Life Technologies, UK) commenced after 3 days of cultivation (10% of the working volume) and was repeated on day 5 (9.1%), day 7 (8.3%), day 9 (7.7%), and day 11 (7.1%). Feeding regimes of the optimization experiment were translated between the scales accordingly.

2.2 | Mixing time measurements

All measurements were performed using a custom-built deep-square well, made from acrylic plastic to allow for visual observations inside the well. The single-well mimic was 16 mm long, 16 mm wide, and 40 mm high, which is dimensionally equivalent to the wells of the micro-Matrix cassette. The well was fixed onto an orbital shaker with 25 mm throw (Sartorius, UK). The color change of a Dual Indictor System for Mixing Time (DISMT) solution was used to determine mixing times inside the well. [18,19] Depending on the pH, the DISMT solution assumes either a red (pH < 6.3), yellow (pH 6.3–8), or green (pH > 8) coloration. The DISMT solution consisted of 64.4 μg L^{-1} Thymol Blue (Fisher Scientific, UK) and 64.8 μg L^{-1} Methyl Red (Fisher Scientific, UK) dissolved in Milli-Q water and was adjusted to neutral pH before use. The well mimic was filled with 2–5 mL of the DISMT solution. Two PHD ULTRA syringe pumps (Harvard Apparatus, USA) were connected to the well through a customized lid to enable the delivery of acid and base while the orbital shaker was in operation. Prior to each experiment, the DISMT solution inside the well was acidified using 20 μL 0.75 M HCl. During the experiment, 20 μL of 0.75 M NaOH was added and the color transition of the liquid from red to yellow was recorded using an iCube high-speed camera (NET New Electronic Technology GmbH, Germany). The time necessary for the solution to reach a homogenous yellow color was reported as the mixing time.

2.3 | Sampling and in-process analytics

Cell counts were performed immediately after sampling using a ViCELL XR (Beckman Coulter, UK). The remaining sample volume was centrifuged at 16,100 × g for 5 min. The supernatant was analyzed for nutrients, metabolites, and dissolved CO_2 using a Bioprofile FLEX (Nova Biomedical, USA). For both analyses, samples were diluted with PBS where appropriate.

The concentration of IgG4 was determined by affinity chromatography using a 1 mL HiTrap Protein G HP column (GE Healthcare, UK) in combination with an Agilent 1200 (Agilent Technologies, UK) high-performance liquid chromatograph (HPLC). Buffer A was prepared from 10 mM NaH_2PO_4 (Fluka, Cat No. 71642-1KG) and 10 mM $NaH_2PO_4 \cdot H_2O$ (Sigma-Aldrich, Cat No. 71507-1KG) and adjusted to pH 7; Buffer B was prepared from 20 mM glycine (VWR, Cat No. 101196X) and adjusted to pH 2.8. The elution peak was recorded via UV absorption at 260 nm and a dilution series of a purified IgG4 standard was used to correlate the resulting peaks with the concentration of IgG4.

2.4 | Glycoprofiling

2.4.1 | N-glycan release

The N-glycans from the IgG4 samples were released using PNGaseF, procainamide labelled and analyzed on a HILIC-FLD-MS platform as

previously described.[20,21] Reagents used for N-glycan release were obtained from the LudgerZyme PNGase F Release Kit (LZ-rPNGaseF-kit, Ludger). Briefly, cell- expressed IgG4 glycoproteins obtained using the different culture methods were dried down. The IgG4 glycoproteins were denatured by adding water (18 μL) and 10x denaturation buffer (2 μL) to the samples, capping the vials tightly and incubating at 99°C for 10 min. Following the denaturation, the samples were allowed to cool to room temperature before adding the following: water (12 μL), 10x reaction buffer (4 μL), 10x NP-40 (2 μL) and PNGaseF (2 μL) and incubating overnight at 37°C. N-glycans were dried with vacuum centrifugation and then converted to aldoses by incubating with 1% formic acid (Sigma) at room temperature for 45 min. The acidified samples were then filtered through a protein binding plate (LC-PBM-96, Ludger). The vials were washed twice with 100 μL water. The washes collected along with the filtrate were dried down in a vacuum centrifuge.

2.4.2 | N-glycan labelling and cleanup

Glycans were labelled with 20 μL of a procainamide solution (containing 10 μL of water) using a LudgerTag Procainamide Glycan Labelling Kit with sodium cyanoborohydride (LT-KPROC-24, Ludger) and incubated for 60 min at 65 °C. Clean up of samples and removal of excess unreacted dye was performed using a HILIC-type clean-up plate (LC-PROC-96, Ludger). Briefly, samples were added to the plate in acetonitrile (230 μL), washed 3 times with acetonitrile (200 μL) and eluted in water (3 $\times$ 100 μL). Purified labelled N-glycans were stored at 4°C until the samples could be processed. For longer term storage -20°C was used.

2.4.3 | HILIC-UHPLC-MS analysis

Procainamide labelled samples and standards were analyzed by liquid chromatography electrospray ionization tandem mass spectrometry (LC-ESI-MS/MS). Procainamide labelled IgG4 glycans were dried using vacuum centrifugation. Samples were resuspended in pure water. Samples were injected in 25% aqueous/75% acetonitrile; injection volume 25 μL. Samples were analyzed by HILIC-LC on an ACQUITY BEH Glycan column (1.7 μm, 2.1 $\times$ 150 mm, Waters Inc, USA) at 40°C on a Dionex Ultimate 3000 UHPLC instrument (Thermo, UK) with a fluorescence detector (λ_{ex} = 310 λ_{em} = 370 nm) coupled in-line to a Bruker AmaZon Speed ETD electrospray mass spectrometer (Bruker Daltonics, Bremen, Germany) directly without splitting, controlled by Bruker HyStar 3.2 and Chromeleon data software version 7.2. Buffer A was 50 mM ammonium formate made from LudgerSep N Buffer stock solution, pH4.4 [LS-N-BUFFX40]; Buffer B was acetonitrile (acetonitrile 190 for UV/gradient quality; Romil #H049). The UHPLC gradient conditions were as follows: 0 to 53.5 min, 76 to 51% B, 0.4 mL min^{-1}; 53.5 to 55.5 min, 51% to 0% B, 0.4–0.2 mL min^{-1}; 55.5 to 57.5 min, 0% B at a flow rate of 0.2 mL min^{-1}; 57.5 to 59.5 min, 0 to 76% B, 0.2 mL min^{-1}; 59.5 to 65.5 min, 76% B, 0.2 mL min^{-1}; 65.5 to 66.5 min, 76% B, 0.2–0.4 mL min^{-1}; 66.5 to 70.0 min, 76% B, 0.4 mL min^{-1}. The Amazon Speed settings used were as follows: scanned samples in maximum resolution mode; positive ion mode; MS scan + three MS/MS scans; source temperature, 250°C; gas flow, 10 L min^{-1}; nebulizer pressure 14.5 psi; capillary voltage, 4500 V; ICC target, 200,000; Max. accu. time (Maximum Accumulation Time), 50.00 ms; rolling average, 2; number of precursor ions selected, 3; release after 0.2 min; mass range scanned, 600–2000; target mass, 900. Mass spectrometry data were analyzed using the Bruker Compass DataAnalysis 4.1 software. LC-ESI-MS/MS chromatogram analysis was performed using Bruker Compass DataAnalysis 4.4 and GlycoWorkbench software. Structures were identified by comparing LC, MS, and MS/MS data.

2.5 | Design of experiment

For the conception of the DoE design and the analysis of the response data, Design Expert v10 (Stat-Ease, USA) was used. A circumscribed central composite design (CCD) was employed to optimize the GS-CHO bolus feeding strategy. The factors total feed volume (in percentage of the initial working volume), feed start (in days after inoculation), and feed rate (in number of bolus additions that the feed volume was divided into) were investigated on five levels. The center point was replicated six times, resulting in 20 runs in total. All parameter combinations were tested in a single experiment, consequently no blocking was necessary. Significant effects were selected through backwards elimination with a cut-off p-value of 0.1.[22] Model analysis with ANOVA ensured model significance, non-significant lack of fit, sufficiently high effect-to-noise ratio, and a difference between adj. R^2 and pred. R^2 no larger than 0.2. Factors and levels are summarized in Table S1.

The bolus feeding regime was optimized for the space-time yield (STY). The STY was calculated at the end of the process using equation 1.[23]

$$STY = \frac{Y}{V \cdot (t - t_0)}, \qquad (1)$$

Where Y is the product yield (mg) at the end of the process, V is the final working volume (L), and $t - t_0$ represents the process duration (d).

3 | RESULTS AND DISCUSSION

3.1 | Mixing time behavior in the micro-Matrix is similar to comparable cell culture systems

An exemplary mixing time experiment within the micro-Matrix well mimic is shown in Figure 1A. In the first frame of the sequence, the drop of base has just detached from the needle and entered the solution, which marked the beginning of the mixing time experiment. The following two frames illustrate how the color transition of the DISMT solution facilitated the identification
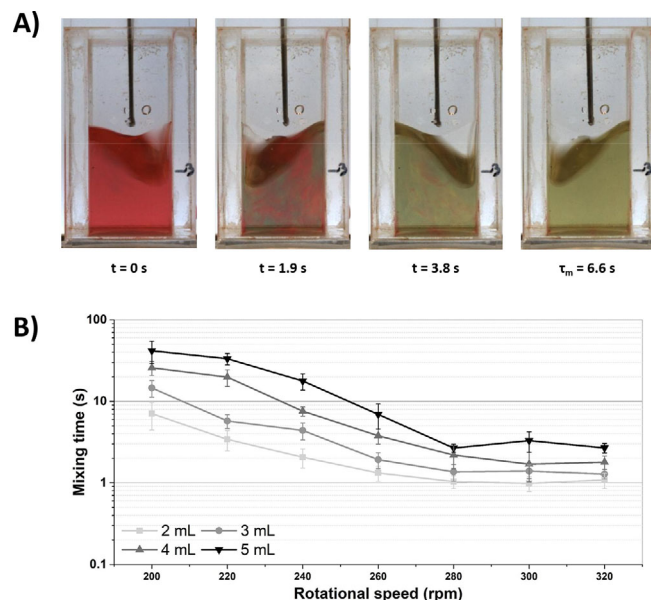
FIGURE 1 (A) Liquid phase motion of an exemplary mixing time experiment at a shaking speed of 240 rpm and a working volume of 4 mL. (B) Mixing time measured inside the micro-Matrix well mimic at varying shaking speeds and working volumes. Data points represent the mean ± SD of 3 to 10 replicates

of poorly mixed zones within the body of liquid. Poorly mixed areas remained either red (acidic) or green (basic) for extended periods of time, whereas well-mixed areas quickly assumed a yellow (neutral) coloration.

At lower shaking speeds, no deformation of the liquid surface could be observed. This behavior was previously described by.[24,25] Once a critical shaking speed is reached, the surface tension of the liquid is overcome, and the surface begins to deform and move in unison with the shaking motion. This critical shaking speed was exceeded for all working volumes at a shaking speed of 200 rpm. Yet, for shaking speeds of 200–220 rpm, mixing was inefficient at the bottom of the well. To prevent concentration gradients and sedimentation of the cells, it was therefore deemed critical to perform cell cultivations at shaking speeds above 220 rpm.

The mixing time was found to range between 0.9 and 41.8 s (Figure 1B). An increased working volume generally led to longer mixing times, whereas increased shaking speeds shortened mixing times. Particularly for a working volume of 5 mL, and contrary to expectations, the mixing time appeared to increase at higher shaking speeds, an effect that has previously been documented for shaken 24 deep-square well plates.[19]

The obtained mixing times fall within the range of comparable microbioreactor and benchtop bioreactor systems. A characterization of the μ24 bioreactor established mixing times of 1–13 s with working volumes of 5 and 7 mL,[15] whereas[26] reported mixing times ranging from 1.7–12,900 s for the 24 SRW format and 10–100 s for a 5 L STR. The ambr 15 was reported to reach mixing times as low as 5 s for a working volume of 13 mL.[27]

3.2 | Rational selection of a scale-down strategy based on matched mixing time and matched CO_2 addition profile

To efficiently employ a small-scale cultivation system for process optimization, a scaling strategy is first devised and then validated by demonstrating that the process outcome is independent of the scale. Here, a benchmark fed-batch process was scaled down from a 5 L STR to the micro-Matrix as well as a 24 SRW microtitre plate format and compared for growth kinetics, productivity, and IgG glycoprofile between scales.

As mammalian cells typically show relatively low requirements for oxygen compared to microbial cells, oxygen mass transfer is generally not a limiting factor.[28] Instead, the scalability of cell culture processes relies more heavily on similar hydrodynamic conditions, which the mixing time can be a useful proxy for. In this study, a matched mixing time of 6 s was chosen as criterion for the scale translation from shaken small-scale systems to the benchtop-scale. It should, however, be noted that mixing at the investigated scales is sufficiently effective at relatively low shaking and stirrer speeds. With an increasing scale, a matched mixing time approach would lead to a drastic increase of the power input in conventional STRs,[29] which could result in unsustainable shear rates. A different scaling parameter should therefore be considered for further scale-up from benchtop STR to pilot- and manufacturing-scale.[30]

Initial experiments (data not shown) indicated that the growth of GS-CHO cells is affected considerably by the percentage of CO_2 in the inflowing gas. Therefore, it was considered critical to maintain a minimum CO_2-fraction of 5% in the inflowing gas between scales. The operating conditions for all scales are summarized in Table S2.

3.3 | Successful scale-down of growth and production kinetics between the micro-Matrix and a 5 L STR

The growth trend was comparable between the 5 L STR and the micro-Matrix (Figure 2A). Furthermore, the maximum VCC did not show significant differences ($p > 0.05$) for these systems. Although the growth of cells cultivated in the 24 SRW was slightly slower, the trend was comparable to the micro-Matrix and 5 L STR system. Similarly, the maximum VCC in the 24 SRW was reached at a later stage of the cultivation but was not significantly different to either micro-Matrix or 5 L STR ($p > 0.05$). The viability (Figure 2B) progressed similarly for all systems until about 8 days post-inoculation. Thereafter, cells grown in the 24 SRW format maintained a high viability with a final value of 89 ± 0.3%, while viabilities in the 5 L STR and the micro-Matrix dropped to 79 ± 1.2% and 62 ± 13.1%, respectively. Particularly, towards the end of the cultivation, the viability of the cells grown in the micro-Matrix showed considerable variability compared to the other systems. This was likely caused by well-to-well variability of the metabolic rates, where wells with higher glycolytic activity showed lower final viabilities (data not shown). By contrast, the final titre was not
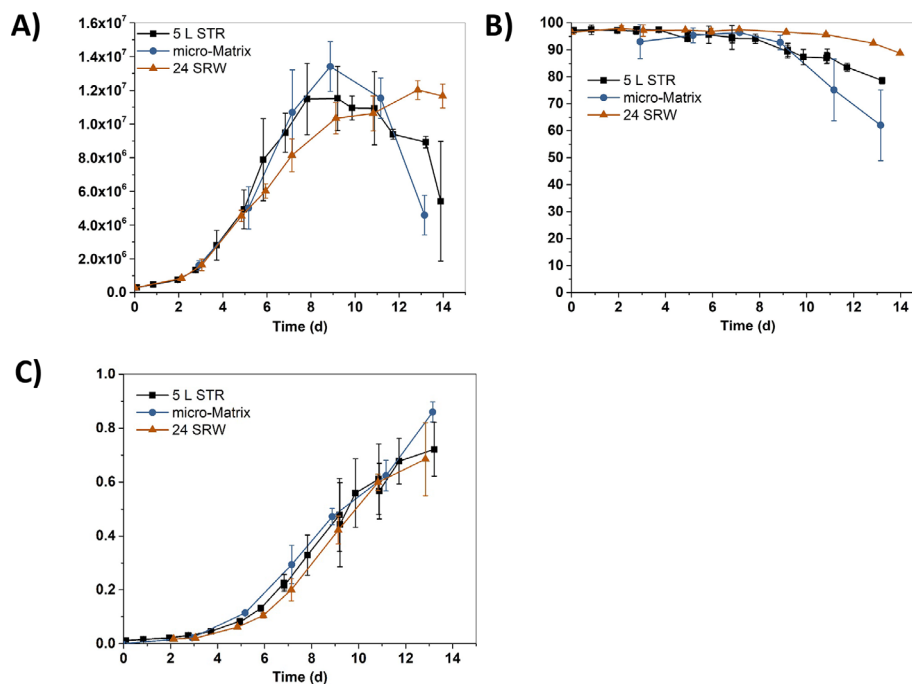
FIGURE 2 Growth and production kinetics of GS-CHO cells grown in a 5 L STR (■), the micro-Matrix (●), and 24 SRW microtitre plates (▲) at a matched mixing time of ∼ 6 s. Data points represent the mean ± SD (5 L STR: $n = 2$, micro-Matrix: $n = 4$, 24 SRW: $n = 6$).

TABLE 1 Growth and production parameters for GS-CHO cells grown at different scales with a matched mixing time of 6 s

Culture parameter	5 L STR	micro-Matrix	24 SRW
Max. VCC (x 10^6 cells mL^{-1} d^{-1})	11.5 ± 1.9	13.4 ± 1.5	12.0 ± 0.6
Cumulative IVCC (x 10^6 cells mL^{-1} d^{-1})	96.5 ± 9.0	91.1 ± 9.3	82.0 ± 2.7
μ_{max} (d^{-1})	0.45 ± 0.04	0.45 ± 0.03	0.40 ± 0.03
Final titre (g L^{-1})	0.72 ± 0.1	0.86 ± 0.04	0.68 ± 0.14
Average q_{mAb} (pg cells^{-1} d^{-1})	7.7 ± 1.3	9.5 ± 0.9	10.6 ± 0.5

Data represent the mean ± SD (5 L STR: $n = 2$, micro-Matrix: $n = 4$, 24 SRW: $n = 6$)

significantly different ($p > 0.05$) between scales for all three systems employed (Figure 2C).

The growth and production parameters summarized in Table 1 further illustrate reasonable agreement between the controlled systems. Notably, the micro-Matrix cultivation resulted in a marginally lower final titre and specific productivity, which was likely caused by the premature onset of cell death compared to the 5 L STR cultivation. Although the 24 SRW format achieved the highest specific productivity, as a result of the comparatively low cumulative integral viable cell concentration (cIVCC), the final titre was lower compared to the other cultivation systems.

3.3.1 | Glycosylation is comparable between controlled cell culture systems

In order to ascertain whether the N-linked glycosylation of the IgG4 was comparable, as the process was scaled, the distribution of key glycosylation features within the glycoprofiles were compared

(Figure 3A-D). The percentage of fucosylated glycans was above 95% at all scales, which was similar to earlier studies of the same cell line and product.[31,32]

Only a small fraction of antibodies (1.3%–3.0%) carried glycans with a bisecting N-acetylglucosamine moiety. Fluctuations between scales were negligible for these glycoprofiles. The distribution of sialylated antibodies was similar for the controlled systems (4.2%–5.7%), but slightly reduced for the 24 SRW format (1.9%). Similarly, galactosylation was comparable for all conditions run in the micro-Matrix and 5 L STR (36.1%–40.6%), but considerably reduced for antibodies that were produced in the 24 SRW (21.4%).

A more detailed representation of the glycoprofiles (Figure 3E and Figure S1) revealed that the most prominent glycan structures found on the IgG4 were a core fucosylated, agalactosylated biantennary glycan (FA2), followed by a core fucosylated, monogalactosylated biantennary glycan (FA2G1) and a core fucosylated, digalactosylated biantennary glycan (FA2G2). Monogalactosylation in the 24 SRW sample was reduced to a similar degree on both arms of the core fucosylated, biantennary glycan (FA2G1), whilst digalactosylation on
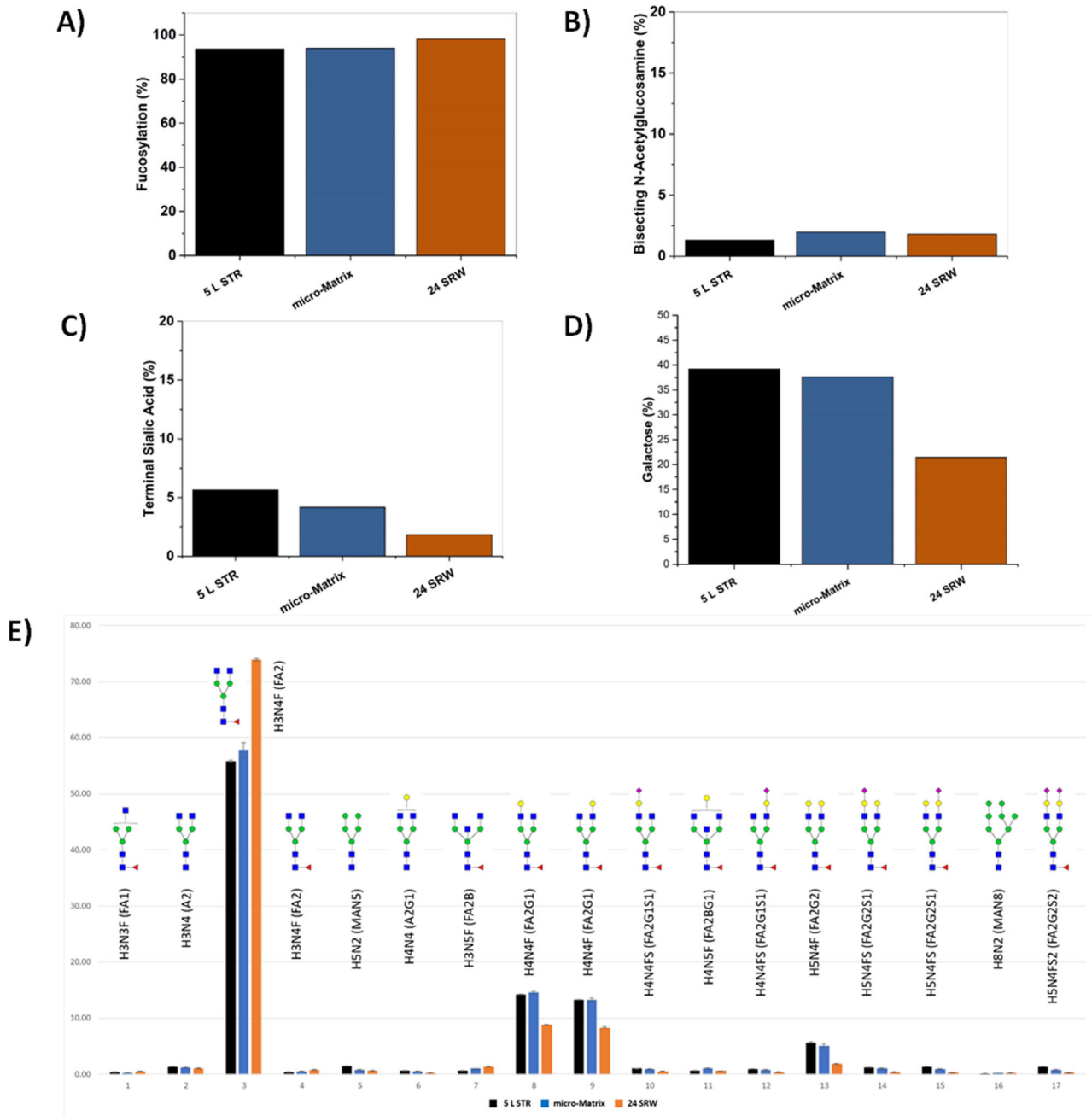
FIGURE 3 Percentage of N-linked glycans of the IgG4 produced in different scales that contain fucose (A), bisecting N-acetylglucosamine (B), sialic acid (C), and galactose (D). (E) Comparison of the relative % areas for each N-glycan peak from each sample analysed; black, 5 L STR; blue, micro-Matrix; orange, 24 SRW. Error bars indicate ± SD. Monosaccharide compositions assigned to peaks from ESI-MS; H = hexose, N = N-acetylhexosamine, F = fucose, S = sialic acid. Possible N-glycan structures are shown in brackets based on MS/MS data: F = fucose, A = antenna, G = galactose, MAN = mannose, S = sialic acid. Red triangle = fucose, blue square = N-acetyl glucosamine, green circle = mannose, yellow circle = galactose, pink diamond = sialic acid

the core fucosylated biattennary glycan (FA2G2) underwent a greater reduction relative to the controlled cultivation formats. As a direct consequence of the fewer available galactose moieties on the 24 SRW sample, terminal sialylation was also decreased.

This difference between the glycoprofiles of the IgG4 samples under the controlled and uncontrolled culture conditions was likely caused by a difference in the pH profile. Cultures in the 24 SRW were not pH

controlled and were therefore subjected to a changing pH environment as illustrated by previous studies that employed pH monitoring in microwell cultivations of CHO cells.[33,34] An effect of the culture pH on the glycoprofile has been reported frequently in the literature but proved highly dependent on the cell line and the investigated glycoprotein. For instance, [35]observed increased galactosylation of an IgG3 produced by hybridoma cells with increasing culture pH,
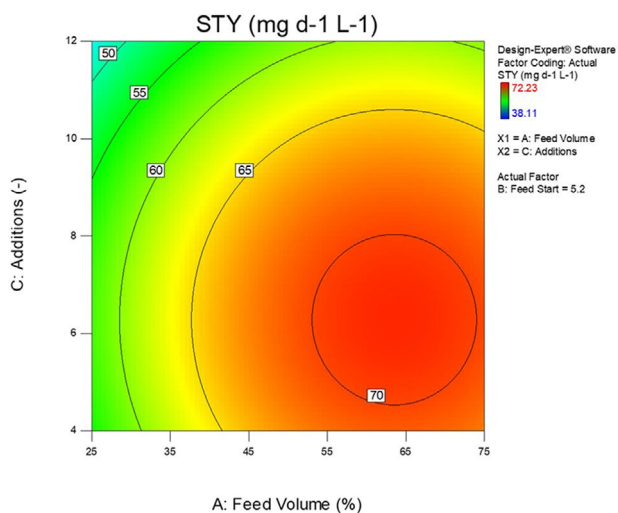
FIGURE 4 Contour plot of the space-time yield (STY) response model. The feed start was set to the predicted optimum of 5.2 days

whereas [36] and [37] reported the opposite effect for a human antibody produced in a human cell line and an IgG1 produced in hybridoma cells, respectively.

The results show that a matched mixing time proved to be a suitable scaling criterion for the process translation from a conventional benchtop-scale stirred bioreactor system to the shaken micro-Matrix microbioreactor. Using the scale-down model then allowed for high-throughput optimization of the feeding regime.

3.4 | Response surface methodology enables rapid optimization of the feeding strategy

The feeding regime of the bolus fed-batch strategy was optimized within the framework of a circumscribed CCD. The star points were used to cover a wider design space. The star points' circumscribed spacing ensured rotatable predictability. The feeding regime was optimized for the STY instead of the final titre to avoid a bias towards long process run times. Using the STY, the process can be optimized for its duration as well as productivity, which can facilitate the identification of processes with high annual productivity given a short turnover.[23] An overview of the tested parameter combinations and their corresponding STY responses is provided in the supporting material (Table S4).

Figure 4 shows the contour plot based on the predictive model of the STY. The model showed good correlation with an adj. R^2 value of 0.81. The factors feed start point and the feed volume were identified as significant model terms. All factors showed a significant quadratic relationship with the STY. An interaction effect was found between the feed start point and the number of feed additions, in which a late feed start favored fewer additions, whereas an early feed start reversed this relationship. An explanation for this interaction could be that in earlier stages of the cultivation the requirements for nutrients were lower than later on in the process. Therefore, small volumes of feed were suf-
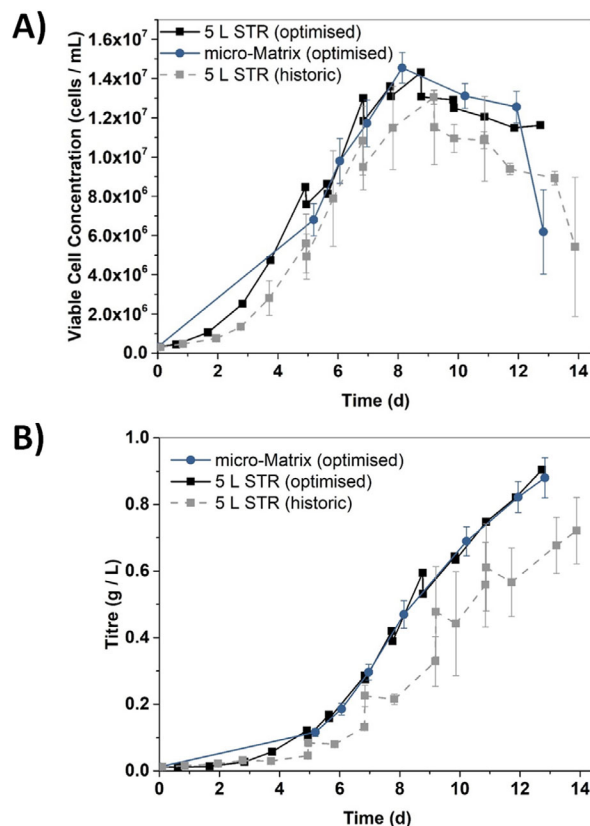

FIGURE 5 Growth (A) and production (B) kinetics of GS-CHO cells grown with the optimized feeding regime in the micro-Matrix (●) and the 5 L STR (■), in comparison to historic data of the cells grown with the original feeding regime in the 5 L STR (▨). Data points represent the mean ± SD (5 L STR optimized: $n = 1$; micro-Matrix optimized: $n = 11$; 5 L STR historic: $n = 2$).

ficient to sustain growth in the beginning, while a more rapid addition was required when feeding commenced late.

The contour plot shows that the optimal STY was captured within the investigated design space. The numerical optimization tool of Design Expert was used to predict the factor combination that yielded the highest STY. The optimal STY of 71 mg d^{-1} L^{-1} was predicted for a feed start after 5 days and a total feed volume of 64% that was divided into six bolus additions to be added on consecutive days.

3.5 | Small-scale model validation and scale up of the optimized feeding strategy show a consistent productivity increase

The predicted optimal bolus feeding regime was repeated in the micro-Matrix for validation and then scaled up to the benchtop scale using the previously established scaling strategy. A comparison to the original fed-batch protocol was made to assess the success of the optimization.

Figure 5 demonstrates minimal differences of the growth kinetics between the scales for the optimized feeding regime. In comparison

TABLE 2 Growth and production parameters of GS-CHO cells grown under optimized and non-optimized feeding regimes at different scales

	5 L STR (optimized)	micro-Matrix (optimized)	5 L STR (historic)
Max. VCC ($\times 10^6$ cells mL^{-1} d^{-1})	14.3	14.5 ± 0.1	11.5 ± 1.9
Cumulative IVCC ($\times 10^6$ cells mL^{-1} d^{-1})	106.5	110.1 ± 0.1	96.5 ± 9.0
μ_{max} (d^{-1})	0.46	0.47 ± 0.01	0.45 ± 0.04
Final titre (g L^{-1})	0.90	0.88 ± 0.06	0.72 ± 0.1
Average q_{mAb} (pg cells^{-1} d^{-1})	8.5	8.0 ± 0.6	7.7 ± 1.3
STY (mg d^{-1} L^{-1})	69.6	67.7 ± 4.6	55.4 ± 4.5

Data represent the mean $\pm$ SD (5 L STR optimized: $n = 1$; micro-Matrix optimized: $n = 11$; 5 L STR historic: $n = 2$)

to the original feeding strategy, a moderate increase of the maximum VCC and a prolonged stationary phase were observed, which led to an increased cIVCC (Table 2). Similarly, the progression of the titre was nearly identical between the scales for the optimized feeding strategy, whereas the original feeding strategy showed a substantially reduced productivity. The final titre of the optimized feeding protocol was 25% higher compared to the original protocol. The optimized feeding strategy in the micro-Matrix and in the 5 L STR resulted in STYs of 67.7 and 69.6 mg d^{-1} L^{-1}, respectively. Through optimization, a 25.4% increase of the STY was achieved compared to the standard protocol.

4 | CONCLUSIONS

This contribution provides a framework for the use of the micro-Matrix system as a cell culture process development tool. Initially, a characterization of the mixing time was performed to gain an understanding of the cultivation environment generated by the system and to further serve as the basis for scale translations. Mixing time was found to be comparable to other microbioreactor systems and benchtop-scale bioreactors and was therefore deemed a suitable scaling criterion.

Based on the information obtained from the mixing time characterization, the mixing time was selected to remain constant between 5 L STR, micro-Matrix and 24 SRW to ensure comparable hydrodynamic conditions. The exemplary scale translation showed similar growth and production kinetics as well as similar glycosylation profiles between micro-Matrix and 5 L STR. The growth profile and the relative % areas of glycan structures differed slightly for cultivations performed in the 24 SRW, which was attributed to the lack of pH control in this format.

The high throughput of the micro-Matrix was then leveraged to optimize the bolus feeding strategy within the framework of a circumscribed CCD. A scale-up of the optimized feeding regime demonstrated analogous growth and production kinetics between the micro-Matrix and the benchtop scale and resulted in a 25.4% increase of the STY compared to the original feeding regime.

Although the discrepancy in both geometry and mode of agitation between the micro-Matrix and conventionally used STRs renders a scale translation between these systems as inherently challenging, equal mixing times proved to be a successful scaling strategy. Subsequent scale-up from benchtop-scale STRs to pilot and manufacturing scale is sufficiently documented in contemporary literature.

AUTHOR CONTRIBUTIONS

V.W.: Conceptualization; data curation; formal analysis; investigation; methodology; writing-original draft; writing-review & editing. F.B.: Conceptualization; funding acquisition; project administration; resources; supervision; writing-review & editing

DATA AVAILABILITY STATEMENT

The data that support the findings of this study are available from the corresponding author upon request.

ORCID

Frank Baganz https://orcid.org/0000-0001-5589-6869

REFERENCES

1. Hemmerich, J., Noack, S., Wiechert, W., & Oldiges, M. (2018). Microbioreactor systems for accelerated bioprocess development. *Biotechnology Journal*, *13*(4), 1700141. https://doi.org/10.1002/biot.201700141.
2. Rao, G., Moreira, A., & Brorson, K. (2009). Disposable bioprocessing: The future has arrived. *Biotechnology Bioengineering*, *102*(2), 348–356. https://doi.org/10.1002/bit.22192.
3. Sandner, V., Pybus, L. P., McCreath, G., & Glassey, J. (2019). Scale-down model development in ambr systems: An industrial perspective. *Biotechnology Journal*, *14*(4), 1700766. https://doi.org/10.1002/biot.201700766.
4. Goldrick, S., Sandner, V., Cheeks, M., Turner, R., Farid, S. S., McCreath, G., & Glassey, J. (2019). Multivariate data analysis methodology to solve data challenges related to scale-up model validation and missing data on a micro-bioreactor system. *Biotechnology Journal*, *15*(3), 1800684. https://doi.org/10.1002/biot.201800684.
5. Bareither, R., & Pollard, D. (2011). A review of advanced small-scale parallel bioreactor technology for accelerated process development: Current state and future need. *Biotechnology Progress*, *27*(1), 2–14. https://doi.org/10.1002/btpr.522.

6. Lattermann, C., & Büchs, J. (2015). Microscale and miniscale fermentation and screening. *Current Opinion in Biotechnology*, *35*, 1–6. https://doi.org/10.1016/j.copbio.2014.12.005.

7. Fenge, C., Klein, C., Heuer, C., Siegel, U., & Fraune, E. (1993). Agitation, aeration and perfusion modules for cell culture bioreactors. *Cytotechnology*, *11*(3), 233–244. https://doi.org/10.1007/BF00749874.

8. Velez-Suberbie, M. L., Betts, J. P. J., Walker, K. L., Robinson, C., Zoro, B., & Keshavarz-Moore, E. (2018). High throughput automated microbial bioreactor system used for clone selection and rapid scale-down process optimization. *Biotechnology Progress*, *34*(1), 58–68. https://doi.org/10.1002/btpr.2534.

9. Xu, S., Hoshan, L., Jiang, R., Gupta, B., Brodean, E., O'Neill, K., Seamans, T. C., Bowers, J., & Chen, H. (2017). A practical approach in bioreactor scale-up and process transfer using a combination of constant P/V and vvm as the criterion. *Biotechnology Progress*, *33*(4), 1146–1159. https://doi.org/10.1002/btpr.2489.

10. Hsu, W.-T., Aulakh, R. P. S., Traul, D. L., & Yuk, I. H. (2012). Advanced microscale bioreactor system: A representative scale-down model for bench-top bioreactors. *Cytotechnology*, *64*(6), 667–678. https://doi.org/10.1007/s10616-012-9446-1.

11. Raval, K., Kato, Y., & Büchs, J. (2007). Comparison of torque method and temperature method for determination of power consumption in disposable shaken bioreactors. *Biochemistry Engineering Journal*, *34*(3), 224–227. https://doi.org/10.1016/j.bej.2006.12.017.

12. Klöckner, W., Tissot, S., Wurm, F., & Büchs, J. (2012). Power input correlation to characterize the hydrodynamics of cylindrical orbitally shaken bioreactors. *Biochemistry Engineering Journal*, *65*, 63–69. https://doi.org/10.1016/J.BEJ.2012.04.007.

13. Büchs, J., Maier, U., Milbradt, C., & Zoels, B. (2000). Power consumption in shaking flasks on rotary shaking machines: I. Power consumption measurement in unbaffled flasks at low liquid viscosity. *Biochemistry Bioengineering*, *68*(6), 589–593.

14. Dürauer, A., Hobiger, S., Walther, C., & Jungbauer, A. (2016). Mixing at the microscale: Power input in shaken microtiter plates. *Biotechnology Journal*, *11*(12), 1539–1549. https://doi.org/10.1002/biot.201600027.

15. Betts, J. P. J., Warr, S. R. C., Finka, G. B., Uden, M., Town, M., Janda, J. M., Baganz, F., & Lye, G. J. (2014). Impact of aeration strategies on fed-batch cell culture kinetics in a single-use 24-well miniature bioreactor. *Biochemistry Engineering Journal*, *82*, 105–116. https://doi.org/10.1016/j.bej.2013.11.010.

16. Silk, N. (2014). High throughput approaches to mammalian cell culture process development [London, UCL (University College London)]. In *Doctoral thesis*. https://discovery.ucl.ac.uk/id/eprint/1420214/

17. Martuza, R. L., Proffitt, M. R., Moore, M. B., & Dohan, C. F. (1976). Evaporation as a cause of positional differences in cell plating and growth in microtiter plates. *Transplantation*, *21*(3), 271–273. https://doi.org/10.1097/00007890-197603000-00016.

18. Melton, L. A., Lipp, C. W., Spradling, R. W., & Paulson, K. A. (2002). Dismt - Determination of mixing time through color changes. *Chemical Engineering Communications*, *189*(3), 322–338. https://doi.org/10.1080/00986440212077.

19. Li, Y., Ducci, A., & Micheletti, M. (2020). Study on mixing characteristics in shaken microwell systems. *Biotechnology Engineering Journal*, *153*, 107392. https://doi.org/10.1016/J.BEJ.2019.107392.

20. Rebello, O. D., Gardner, R. A., Urbanowicz, P. A., Bolam, D. N., Crouch, L. I., Falck, D., & Spencer, D. I. R. (2020). A novel glycosidase plate-based assay for the quantification of galactosylation and sialylation on human IgG. *Glycoconjugate Journal*, *37*(6), 691–702. https://doi.org/10.1007/s10719-020-09953-9.

21. Kozak, R. P., Tortosa, C. B., Fernandes, D. L., & Spencer, D. I. R. (2015). Comparison of procainamide and 2-aminobenzamide labeling for profiling and identification of glycans by liquid chromatography with fluorescence detection coupled to electrospray ionization-"mass spectrometry. *Analytical Biochemistry*, *486*, 38–40. https://doi.org/10.1016/j.ab.2015.06.006.

22. Guy, H. M., McCloskey, L., Lye, G. J., Mitrophanous, K. A., & Mukhopadhyay, T. K. (2013). Characterization of lentiviral vector production using microwell suspension cultures of HEK293T-derived producer cells. *Human Gene Therapy Methods*, *24*(2), 125–139. https://doi.org/10.1089/hgtb.2012.200.

23. Bausch, M., Schultheiss, C., & Sieck, J. B. (2019). Recommendations for comparison of productivity between fed-batch and perfusion processes. *Biotechnology Journal*, *14*(2), 1700721. https://doi.org/10.1002/biot.201700721.

24. Doig, S. D., Pickering, S. C. R., Lye, G. J., & Baganz, F. (2005). Modelling surface aeration rates in shaken microtitre plates using dimensionless groups. *Chemical Engineering Science*, *60*(10), 2741–2750. https://doi.org/10.1016/j.ces.2004.12.025.

25. Hermann, R., Lehmann, M., & Büchs, J. (2003). Characterization of gas-liquid mass transfer phenomena in microtiter plates. *Biotechnology Bioengineering*, *81*(2), 178–186. https://doi.org/10.1002/bit.10456.

26. Barrett, T. A., Wu, A., Zhang, H., Levy, M. S., & Lye, G. J. (2010). Microwell engineering characterization for mammalian cell culture process development. *Biotechnology Bioengineering*, *105*(2), 260–275. https://doi.org/10.1002/bit.22531.

27. Nienow, A. W., Rielly, C. D., Brosnan, K., Bargh, N., Lee, K., Coopman, K., & Hewitt, C. J. (2013). The physical characterisation of a microscale parallel bioreactor platform with an industrial CHO cell line expressing an IgG4. *Biochemistry Engineering Journal*, *76*, 25–36. https://doi.org/10.1016/j.bej.2013.04.011.

28. Lavery, M., & Nienow, A. W. (1987). Oxygen transfer in animal cell culture medium. *Biochemistry Bioengineering*, *30*(3), 368–373. https://doi.org/10.1002/bit.260300307.

29. Tissot, S., Farhat, M., Hacker, D. L., Anderlei, T., Kühner, M., Comninellis, C., & Wurm, F. (2010). Determination of a scale-up factor from mixing time studies in orbitally shaken bioreactors. *Biochemistry Engineering Journal*, *52*(2–3), 181–186. https://doi.org/10.1016/J.BEJ.2010.08.005.

30. Xing, Z., Kenty, B. M., Li, Z. J., & Lee, S. S. (2009). Scale-up analysis for a CHO cell culture process in large-scale bioreactors. *Biochemistry Bioengineering*, *103*(4), 733–746. https://doi.org/10.1002/bit.22287.

31. VelezSuberbie, M. L., Tarrant, R. D. R., Tait, A. S., Spencer, D. I. R., & Bracewell, D. G. (2013). Impact of aeration strategy on CHO cell performance during antibody production. *Biotechnology Progress*, *29*(1), 116–126. https://doi.org/10.1002/btpr.1647.

32. Tait, A. S., Tarrant, R. D. R., Velez-Suberbie, M. L., Spencer, D. I. R., & Bracewell, D. G. (2013). Differential response in downstream processing of CHO cells grown under mild hypothermic conditions. *Biotechnology Progress*, *29*(3), 688–696. https://doi.org/10.1002/btpr.1726.

33. Naciri, M., Kuystermans, D., & Al-Rubeai, M. (2008). Monitoring pH and dissolved oxygen in mammalian cell culture using optical sensors. *Cytotechnology*, *57*(3), 245–250. https://doi.org/10.1007/s10616-008-9160-1.

34. Toussaint, C., Henry, O., & Durocher, Y. (2016). Metabolic engineering of CHO cells to alter lactate metabolism during fed-batch cultures. *Journal of Biotechnology*, *217*, 122–131. https://doi.org/10.1016/J.JBIOTEC.2015.11.010.

35. Müthing, J., Kemminer, S. E., Conradt, H. S., Šagi, D., Nimtz, M., Kärst, U., & Peter-Katalinić, J. (2003). Effects of buffering conditions and culture pH on production rates and glycosylation of clinical phase I anti-melanoma mouse IgG3 monoclonal antibody R24. *Biotechnology Bioengineering*, *83*(3), 321–334. https://doi.org/10.1002/bit.10673.

36. Seo, J. S., Kim, Y. J., Cho, J. M., Baek, E., & Lee, G. M. (2013). Effect of culture pH on recombinant antibody production by a new human cell line, F2N78, grown in suspension at 33.0 °C and 37.0 °C. *Applied Microbiology and Biotechnology*, *97*(12), 5283–5291. https://doi.org/10.1007/s00253-013-4849-2.

37. Ivarsson, M., Villiger, T. K., Morbidelli, M., & Soos, M. (2014). Evaluating the impact of cell culture process parameters on monoclonal antibody N-glycosylation. *Journal of Biotechnology*, *188*, 88–96. https://doi.org/10.1016/J.JBIOTEC.2014.08.026.

SUPPORTING INFORMATION

Additional supporting information may be found in the online version of the article at the publisher's website.